Title: Error causes a perceived pull to the present in evolutionary rates

Authors: Brian C. O'Meara[1*] and Jeremy M. Beaulieu[2]

Affiliations:

[1]Department of Ecology and Evolutionary Biology, University of Tennessee; Knoxville, Tennessee, 37996-1610 USA.

[2]Department of Biological Sciences, University of Arkansas; Fayetteville, Arkansas, 72701 USA.

*Corresponding author. Email: bomeara@utk.edu

Abstract: Interpretations of biodiversity patterns across timescales necessarily assume that fundamental processes of evolution do not change over time. A recurring pattern across a variety of biological datasets, from genomes to the fossil record, has shown evolutionary rates increasing toward the present or over shorter time scales, however, indicating potentially fundamental but unknown processes unifying evolutionary timescales. We demonstrate that these patterns are statistical artifacts of time-independent errors present across ecological and evolutionary datasets, which produce hyperbolic patterns of rates through time. Specifically, no matter how time-independent error and measurements of evolutionary change are distributed, estimated rates exhibit a hyperbolic pattern when plotted against time. Our findings validate assumptions of uniformitarianism but pose new challenges for the rate estimates foundational to other macroevolutionary models.

One-Sentence Summary: Errors in ecological and evolutionary data lead to observed patterns of increasing macroevolutionary rates toward the present.

Main Text:

The diverse array of processes across organisms, time, and space serves as a testament to the dynamic nature of evolution, where few universal rules persist. Consequently, biologists take immediate notice when broad patterns manifest across a diverse set of lineages. One such recurring pattern is that evolutionary rates exhibit an exponential increase towards the present, highlighting a potentially new fundamental principle in the unfolding narrative of life's progression. The consistency of this pattern across dimensions of diversity, from genomes to the fossil record (*1-4*), highlight its universality and points to the need for new conceptual bridges connecting disparate timescales of evolutionary change (*5*). It also challenges the long-held view that the processes playing out in the past generally behave similarly in the present. Reconciling this pattern offers the potential for new insights into the underlying mechanisms that shape biodiversity.

Within this context, however, these patterns are potentially an inherent artifact resulting from a rate expressed as a ratio of evolutionary change and time (*6, 7*). The concern over spurious correlations between ratios and shared factors has a longstanding history in the statistical literature, dating back to Pearson's pioneering work more than a century ago (*8*). Pearson illustrated this problem by recounting a biologist's study of skeletal measurements, specifically femur and tibia length normalized as fractions of the humerus length. Expecting a high correlation to validate correct groupings, the biologist was unaware that an "imp" had randomly shuffled bones between specimens. Surprisingly, the high correlation persisted even after this randomization, revealing that such spurious relationships arise from inherent properties of the variables rather than indicating meaningful biological connections (*8-10*).

Similarly, when plotting an evolutionary rate against its corresponding denominator, time, the representation becomes a plot of time against its reciprocal (i.e., 1/time), resulting in a relationship that is negatively biased (*6, 7*). In fact, if the numerator is held constant, the slope on a log-log scale must be -1.0 (*1, 11*). However, the numerator in an evolutionary rate, which quantifies the absolute amount of evolutionary change, is unlikely to remain constant across all timescales (*7*). A study emphasized this point by showing that the amount of evolutionary change remains constant over a predictable interval of time until substantial "bursts" of evolutionary change occur (*12*).

One potentially crucial but overlooked factor affecting rate patterns is the impact of empirical biases and errors inherent in rate estimates. Many of these biases, when scaled by time, may drive rates to follow a hyperbolic trend, potentially asymptoting above zero across deeper time scales. This, too, aligns with existing literature describing patterns and hypothesizing about causes (*1, 5, 11*). Here we introduce a set of novel models that assess the relationship between rate and time that includes hyperbolic and linear functions of time. We also unleash an "imp" of our own with an innovative randomization procedure that breaks down rates into numerator and denominator components, reshuffles the numerator with respect to time, then recalculates the rate. By refitting our models to these random datasets, we illustrate the artifactual nature of rates exponentially increasing towards the present.

Components of Evolutionary Rate Patterns Through Time

In the context of evolutionary biology, a rate is a measure of evolutionary change per unit of time,

$$r(t) = \frac{x(t)}{t}.$$

Evolutionary change, $x(t)$, encompasses a variety of measures, including number of nucleotide substitutions in DNA (*13*), the number of transitions between discrete phenotypes (*14*), speciation and extinction events (*15*), or the absolute change in a continuous trait up until time, t (*16*). The specifics of the different types of evolutionary rates and how they are estimated are intricate. For instance, one rate may assume changes follow a Poisson distribution on a nested tree structure (e.g., substitution rates), while others may assume trait changes are drawn from a normal distribution with the rate being the measure of the variance (e.g., Brownian motion). Nevertheless, at its core, an evolutionary rate reduces to some measure of change over time.

While it is common to perceive uncertainty and error as obscuring patterns rather than contributing to them, these uncertainties and errors may be key drivers of the repeated pattern of rates increasing towards the present. For illustrative purposes, we focus on the simplest approach for calculating rates of morphological evolution to demonstrate the impact of biases and errors on the relationship between rate and time. Measurements are assembled as a set of paired comparisons that differ in some trait value (e.g., body size) measured at two separate time points, with ratio of the differences in trait and time being an estimate of the rate,

$$\hat{r}(t) = \frac{|x_2 - x_1|}{t_2 - t_1}, t_2 > t_1.$$

Here x_1 and x_2 are the initial and final values of the trait measurement between two time points, t_1 and t_2, respectively. Expressing a rate in such a way is similar to the "darwin," a widely used unit of evolutionary change first defined by Haldane (*17*).

Various phenomenological patterns can describe how rates change through time. The simplest is that $\hat{r}(t)$ exhibits a constant rate of change, maintaining an expected value regardless of the measurement interval. For example, a mutation rate resulting from DNA copying errors might be anticipated to be consistent when scaling the number of mutations by time within clades of different ages. In other words, even though a clade with a crown age of 5 million years is expected to have far fewer mutations than a 50-million-year-old clade, on a per-time basis the rate will be identical. The biological rationale for such consistency in rate is rooted in the assumption that processes governing rates operate similarly in the past as they do in the present – a foundational premise in much of evolutionary biology. On the other hand, a significant secular change in the mutation rate might result from a general enhancement in DNA copying or repair mechanisms. Thus, we might expect differences between x_2 and x_1 to decrease near the present.

Measurements of x_i often reflect the mean for a species and, therefore, represent an estimate of the true value. If each measurement estimate, x_i, carries some level of noise attributed to factors like finite sample size or measurement error, then $\widehat{x_i} = x_i + \varepsilon_i$, with ε_i denoting an error component that can lead to overestimation or underestimation of the overall rate. Thus, we can express the rate estimate as including error:

$$\hat{r}(t) = \frac{|(x_2 + \varepsilon_2) - (x_1 + \varepsilon_1)|}{t_2 - t_1}, t_2 > t_1.$$

The impact of an explicit error component is readily seen if we assume no differences in the trait measurements, such that $x_2 - x_1 = 0$. This reduces a rate estimate as being the difference between the two error terms,

$$\hat{r}(t) = \frac{|\varepsilon_2 - \varepsilon_1)|}{t_2 - t_1}, t_2 > t_1.$$

Since these errors are not inherently time-dependent (e.g., sequencing errors in a DNA analysis), there are no *a priori* reasons for the magnitude of the error in a 5-million-year-old clade would necessarily be any greater or lesser than the magnitude in a 50-million-year-old clade. Thus, a hyperbola will invariably result when the ratio of these differences in error are scaled by time, and then plotted against time. The impact of uncertainty and error is particularly pronounced in models such as those applied to DNA evolution, where differences between taxa are presumed to be changes occurring along branches in a phylogenetic tree. Sequencing errors independent of time can introduce not only an upward bias in the rate but also a bias favoring a hyperbolic relationship between rate and time (*2*). If a constant rate exists, such as from a molecular clock or net diversification, its impact outweighs errors over extended periods (Fig. 1).

To assess the relative contribution of constant, hyperbolic, and linear functions towards a rate estimate over time, we derived a novel least-squares approach. Our method allowed us to predict changes in observed evolutionary rates sampled through time by minimizing the logarithm of the residual sum of squares between the predicted and observed values (*18*). We derived a model that, at its most complex, is given as,

$$\hat{r}(t) = \frac{h}{t} + mt + b.$$

Here h denotes the hyperbolic component [in units of $x(t)$], m is scalar modulating the effect of time up and down linearly [in units of $x(t)t^{-2}$], and b is a constant base rate [in units of $x(t)t^{-1}$]. The full model assumes all three components have impacted the fitted value for $\hat{r}(t)$ in some way. We also fit a range of restrictions to this model where one or more of the parameters are set to zero. For example, restricting h=m=0 is a model in which the rates would be inferred to be constant through time, as one would expect from a process like a molecular clock. The maximum likelihood fit of a model was assessed using the logarithm of the residual sum of squares and first converting this into a measure of the model variance and then into a log-likelihood. To facilitate comparisons across a set of models, we converted the log-likelihood into an Akaike Information Criterion score (AIC); we also assessed confidence regions (e.g., figs. S1-6) around each of the parameters (*18*).

Revisiting Empirical Cases of Age-Dependent Rates

We analyzed five empirical datasets that encompass diverse data types, including substitution rates [Ho *et al.*, (*2*)], rates of body size evolution from extant and extinct taxa [measured in darwins; Gingerich, (*1*), Uyeda *et al.*, (*12*)], speciation rates from phylogenetic trees of extant species [Henao Diaz *et al.*, (*3*)], and contemporary species extinction rates [Barnosky *et al.*, (*19*)]. We also included a dataset of birth rates obtained from 25,000 trees simulated under a Yule process (i.e., pure birth) with the same rate (i.e., 0.10 birth Myr^{-1}) and clade ages drawn from a uniform distribution. Estimates of the birth rates included a correction to account for the biased estimates for smaller tree sizes (see *18*). This simulated dataset served as a type of control given that the trees were generated without error and thus the best fit model should generally appear as a horizontal line centered on the generating rate.

In all five empirical datasets, we observed a consistent negative trend in rates through time on a log-log scale (Fig. 1). This aligns with published results indicating higher rates closer to the present, declining as time increases. When we fit our least-squares model separately to each empirical dataset, we found, with one exception, that all were best fit by a model that

included all three parameters (*h*, *m*, and *b*). The Henao Diaz *et al*. (*3*) data favored a model without a base rate (b = 0 speciation events Myr^{-1}), but there were three other models within 2 AIC units from the best fit model, including the full model, and all featured a positive hyperbolic parameter estimate ($\hat{h}$ = 1.71-2.07 speciation events). One consistent finding across all five empirical datasets was that the best fit model included a positive hyperbolic parameter estimate ($\hat{h} > 0$) as well as a non-zero linear component ($\hat{m} \neq 0$).

For the fitted rate values within each dataset, we decomposed the rate to reflect the proportion attributed to each of the three components in our least-squares model. This allowed us to assess how much of the fitted rate comes from each component as a function of time instead of relying solely on interpreting the parameters in the fitted model. This revealed, for example, which portions of the overall model fit were predominantly driven by a linear trend in the rates even in the presence of a non-zero hyperbolic component (*18*).

Decomposing the fitted rates in this way revealed that a significant portion of the relationship between rate and time in the empirical datasets is strongly influenced by the hyperbolic component (Fig. 1). This occurred despite model fits indicating that there was signal for both constant and linear components. Interestingly, in the case of body size evolution datasets of Gingrich (*1*) and Uyeda *et al*. (*12*), the hyperbolic component was replaced by the constant component, followed by a small remaining portion showing the linear component as having a substantial contribution to the rate (Fig. 1). Putting these linear trends in the context of the estimate of the *m* parameter, there is a signal for rates of body size evolution to decrease as time increases that contributes strongest to the deepest time points [Gingerich (*1*): $\hat{m}$ = -0.00007 (CI: -0.00009:-0.00005) Δlog body mass per Myr^{-2}; Uyeda *et al*. (*12*): $\hat{m}$ = -0.0005 (CI: -0.0006:-0.0005) Δlog body mass per Myr^{-2}]. Similarly, the speciation rates of Henao Diaz *et al*. (*3*) shifted from a predominant signal for the hyperbolic component to the linear component being the strongest contributor towards the rate for the oldest clades. The linear component indicated a trend of speciation rates increasing across these deep time scales [$\hat{m}$ = 0.00002 (CI: -0.00001:0.00004) speciation events per Myr^{-2}; Fig. 1], though the confidence interval includes zero and at the maximum time only raises the speciation rate by 0.008 events per Myr^{-2}. Moreover, for all the empirical datasets, the simplest *h*00 model, which uses only a hyperbolic component, has only a slightly worse coefficient of determination than the best fitting models, even if there is a substantial difference in AIC (table S1).

Notable exceptions were the datasets of Ho *et al*. (*2*) and Barnosky *et al*. (*19*), which showed no strong contribution by the linear component. In both cases, the hyperbolic component contributed strongest nearer the present, with the remainder mostly favoring constant rates. There was substantial uncertainty not just in the parameter estimates for these datasets (figs S5-6; table S1), but also which component contributed to the fitted rate generally, which we suspect was due to the small sample sizes of these datasets (n=17 and n=11, respectively). In the pure birth simulation, the overall trend was a horizontal trend line driven almost exclusively by the constant component, as expected, which was centered near the generating rate in our simulation ($\hat{b}$ = 0.106 (CI: 0.103:0.109) birth events Myr^{-1} vs b_{true} = 0.10 birth events Myr^{-1}).

Deriving an appropriate null expectation

The strong contribution of the hyperbolic component does not rule out the possibility that a biological process could underlie the increasing rates towards the present. For example, for rates of body size evolution there might exist a finite range of viable body sizes for terrestrial vertebrates, with the potential for doubling over short time scales but reaching a fixed maximum

numerator over longer periods. The traditional null expectation assumes no relationship between rate and time and is represented by a horizontal line. However, this null expectation makes a strong assumption that the amount of reconstructed evolutionary change, $x(t)$, is perfectly correlated with reconstructed time. We expect some degree of imperfect correlation, i.e., at its most extreme, the evolutionary change could be entirely random in relation to time. In such instances, we are plotting random rates against time, which manifests exactly as a hyperbola.

To generate a new empirical null, we first separated each empirical rate into its numerator and denominator components. The numerator was obtained either directly from the original data, or by multiplying the empirical rate by their respective denominator of measured time. We then shuffled the numerators at random across a given empirical dataset and divided them by the unshuffled times to obtain a new set of rates and times. This not only follows the long tradition of using reshuffling to get null distributions when examining ratios against common factors (*8*), but also has the advantage of keeping the same distributions of times and amount of change as the original data, which can matter for some of the biases here [i.e., (*9*)]. Our expectation was that the observed relationships between rate and time will differ from results where evolutionary change and time are completely random with respect to one another.

As expected, when we randomized the numerator relative to the denominator of the empirical rates, the relationship between rate and time was solely driven by the hyperbolic component across all examined datasets (Fig. 2, OR comparison type). However, we also surprisingly observed substantial similarity between the randomized and empirical results. They were so similar, in fact, that when model parameters were optimized on the randomized data and applied to the corresponding empirical data, the resulting coefficient of determination (R^2), which indicates explanatory power, was nearly identical or sometimes greater than that of the actual empirical fit (Fig. 2). For example, in our largest empirical dataset, Uyeda *et al*. (*12*) with 5,886 observations, we predicted 86.9% of the variation using an *hmb* model fit to the actual data, but fitting to randomized data explains on average 85.6% of the variation.

We hasten to acknowledge that some differences in the R^2 among empirical and randomized fits is expected given the inferred shifts in the contribution of three components through time. For example, while the empirical dataset of Uyeda *et al*. (*12*) is largely consistent with a hyperbolic distribution (Fig. 1), the rates nearer the maximum age are largely driven by the linear component. Nevertheless, as a practical matter, the fact that we can take measurements like amount of change within *Daphnia* over a summer (*20*), the amount of change between late Cretaceous *Tyrannosaurus* and Triassic *Coleophysis* over 98 million years (21), and many datasets in between, shuffle these values, and have the model fit nearly as well on the original data—including explaining over 80% of the variation—suggests that the apparent patterns arise from fitting noise. By contrast, the Yule dataset, where there is variance due to the model (a given simulation condition can create trees of very different sizes) but no error in the number of taxa used, the tree, or the total height. In this case, the empirical pattern was very different from a hyperbola. Even an error creating a bias, such as censoring the data with zero rates without using a correction, creates a pattern very different from the hyperbola as a consequence of noise (fig. S7).

Discussion

Our study demonstrates that the pattern of increased evolutionary rates towards the present, observed across various axes of biodiversity, such as contemporary extinction rates (*19*) and macroevolutionary rates in morphology and molecular studies (*1, 2, 12*), closely resembles what we would expect from purely random data. Even within large datasets, the observed hyperbolic

pattern closely mirrors noise, except for certain periods where a signal-to-noise ratio would suggest constancy in rates. Furthermore, it is worth noting that while our focus was on ecological and evolutionary datasets, similar conflicts between rates measured over different time scales exist in other fields, including the Hubble tension regarding the cosmic expansion rate (*22*). For instance, incorporating Milky Way Cepheids, stars whose brightness fluctuates radially over time, instead of distant stars, increases the expansion estimate (*23*), aligning with our expectations. However, delving into the specifics of the expansion's timing and scale, rather than solely focusing on its antiquity, is beyond the scope of the work presented here.

Our findings do not imply that assessing patterns of rates over time is impossible. For instance, in dendrochronology, annual tree growth is often estimated using cores with a relatively consistent number of years, rather than increasing the number of years for older samples. A recent study on contemporary bird extinction dynamics (*24*) employed 100-year rolling windows to estimate average extinction rates over time, and contrary to expectation, did not find the highest rate at present. Approaches like these, which maintain consistent time intervals, minimize the likelihood of secular trends in time as well as numerator errors and are likely robust to the statistical artifacts uncovered here.

An important implication of our results is that any errors present in measurements of evolutionary change not only greatly affect rate estimation overall, but also any comparative test that examines rate shifts within a single phylogenetic tree. Consider a scenario where we want to compare evolutionary rates between two clades, with one nested within the other and thus differing in their overall crown age. Any inaccuracies in trait measurements or character state assignments within the tree could lead to the erroneous inference that the younger clade has a higher rate, simply due to less overall time in terms of branch lengths to mitigate the effects of these errors (fig. S10). This discrepancy also creates a concerning disconnect between the expected error rates for specific phylogenetic comparative models, derived from simulations, and their actual behavior in empirical settings when assessing rate differences within and among clades. That is, null models for many comparative tests may fit far worse in an empirical setting than might be indicated by careful simulation study conducted in the absence of measurement error (*25*), providing alternative explanations with artificially inflated support. Even with Bayesian approaches that attempt to integrate over uncertainty in results, data are still typically assumed to be free of errors, and this being incorrect will tend to lead to increased rates, especially where the magnitude of the effect of the error is high relative to the magnitude of the effect of the signal.

We anticipate that our findings will encourage further development of approaches that acknowledge measurement error when estimating rates. In models of continuous trait evolution, measurement error can be addressed by directly inputting the standard error of the species' mean for a trait to the model (*26*). However, this practice is not yet standard, but at the very least, measurement error could be incorporated as a parameter of the model. In other comparative models, especially those related to the evolution of discrete characters (e.g., nucleotides or higher-level phenotypic characters exhibiting a finite state space), rates are determined without methods to mitigate potential errors, like inaccuracies in character state assignments. Such errors have a clear impact of inflating rates over shorter time scales (e.g., Fig. 1 and fig. S9).

One unexplored issue is that while our study solely focused on errors in measurements of evolutionary change, errors in the temporal component underlying a rate can also significantly influence rate estimates. In certain scenarios, such as diversification models, we suspect errors in branch lengths might counteract the observed patterns, at least partially. Therefore, given the potential biases in molecular age estimates (*27-29*), it is prudent to prioritize the development of

integrative approaches that address errors not only in measurements of evolutionary change, but also in the underlying branch lengths.

Finally, our findings demonstrate the importance of using informed nulls as expectations of a process (see *30*), especially as errors have a biased effect on rate estimates. Understanding how rates vary both within and among phylogenies will always remain a key part of biology, as they can point to important principles governing biodiversity across disparate timescales. However, statistical artifacts can still impishly affect our results, particularly when we dismiss uncertainties in our measurements as inconsequential.

References and Notes

1. P. D. Gingerich, Rates of evolution: effects of time and temporal scaling. *Science* **222**, 159-161 (1983). doi: https://www.science.org/doi/10.1126/science.222.4620.159.
2. S. Y. W. Ho, M. J. Phillips, A. Cooper, A. J. Drummond, Time dependency of molecular rate estimates and systematic overestimation of recent divergence times. *Molecular Biology and Evolution* **22**, 1561-1568 (2005). doi: https://doi.org/10.1093/molbev/msi145.
3. L. Henao Diaz, L. J. Harmon, M. T. C. Sugawara, M. W. Pennell. 2019. Macroevolutionary diversification rates show time dependency. *Proceedings of the National Academy of Sciences, U.S.A.* **116**, 7403-7408 (2019). doi: https://doi.org/10.1073/pnas.1818058116.
4. L. J. Harmon, M. W. Pennell, L. F. Henao Diaz, J. Rolland, B. N. Sipley, J. C. Uyeda, Causes and consequences of apparent time scaling across all estimated evolutionary rates. *Annual Review of Ecology, Evolution, and Systematics* **52**, 587-609 (2021). doi: https://doi.org/10.1146/annurev-ecolsys-011921-023644.
5. J. Rolland, L. F. Henao-Diaz, M. Doebeli, R. Germain, L. J. Harmon, L. L. Knowles, L. H. Low, J. E. Mank, A. Machac, S. P. Otto, M. Pennell, N. Salamin, D. Silvestro, M. Sugawara, J. Uyeda, C. E. Wagner, D. Schluter, Conceptual and empirical bridges between micro- and macroevolution. *Nature Ecology and Evolution* **7**, 1181-1193 (2023). doi: https://doi.org/10.1038/s41559-023-02116-7.
6. A. Hallam, Evolutionary size increase and longevity in Jurassic bivalves and ammonites. Nature 258, 493-496 (1975). doi: https://doi.org/10.1038/258493a0.
7. S. J. Gould, Smooth curve of evolutionary rate: a psychological and mathematical artifact. *Science* **226**, 994-996 (1983). doi: https://www.science.org/doi/10.1126/science.6505682.
8. K. Pearson, Mathematical contributions to the theory of evolution.—On a form of spurious correlation which may arise when indices are used in the measurement of organs. *Proceedings of the Royal Society, London* **60**, 359-367 (1897). doi: https://doi.org/10.1098/rspl.1896.0076.
9. F. Chayes, On ratio correlation in petrography. *Journal of Geology* **57**, 239-254 (1949). doi: https://doi.org/10.1086/625606.
10. W. R. Atchley, C. T. Gaskins, D. Anderson, Statistical properties of ratios. I. Empirical results. *Systematic Biology* **25**, 137-148 (1976). doi: https://doi.org/10.2307/2412740.
11. S. P. De Lisle, E. I. Svensson, Evolutionary change is remarkably constant across timescales. bioRxiv [Preprint] (2023). doi: https://doi.org/10.1101/2023.12.02.569704.

12. J. C. Uyeda, T. F. Hansen, S. J. Arnold, J. Pienaar, The million-year wait for macroevolution bursts. *Proceedings of the National Academy of Sciences, U.S.A.* **108**, 15908-15913 (2011). doi: https://doi.org/10.1073/pnas.1014503108.

13. T. H. Jukes, C. R. Cantor, "Evolution of protein molecules" in *Mammalian Protein Metabolism* (Academic Press, New York), pp. 21-132. doi: http://dx.doi.org/10.1016/B978-1-4832-3211-9.50009-7.

14. M. Pagel, Detecting correlated evolution on phylogenies: a general method for the comparative analysis of discrete characters. *Proceedings of the Royal Society, London* **255**, 37-45 (1994). doi: https://doi.org/10.1098/rspb.1994.0006.

15. S. Nee, R. M. May, P. H. Harvey, The reconstructed evolutionary process. *Philosophical Transactions of the Royal Society, London* **344**, 305-311 (1994). doi: https://doi.org/10.1098/rstb.1994.0068.

16. J. Felsenstein, Phylogenies and the comparative method. American Naturalist 125, 1-15 (1985). doi: https://www.jstor.org/stable/2461605.

17. J. B. S. Haldane, Suggestions as to the quantitative measurement of rates of evolution. *Evolution* **3**, 51-56 (1949). doi: https://doi.org/10.2307/2405451.

18. Materials and methods are available as supplementary materials.

19. A. D. Barnosky, N. Matzke, S. Tomiya, G. O. U. Wogen, B. Swartz, T. B. Quental, C. Marshall, J. L. McGuire, E. L. Lindsey, K. C. Maguire, B. Mersey, E. A. Ferrer, Has the Earth's sixth mass extinction already arrived? *Nature* **471**, 51-57 (2011). doi: https://doi.org/10.1038/nature09678.

20. A. J. Tessier, A. Young, M. Leibold, Population dynamics and body-size selection in *Daphnia*. *Limnology and Oceanography* **37**, 1-13 (1992). doi: https://doi.org/10.4319/lo.1992.37.1.0001.

21. E. H. Colbert, Evolution of horned dinosaurs. *Evolution* **2**, 145-163 (1948). doi: https://doi.org/10.1111/j.1558-5646.1948.tb02737.x.

22. M. Kamionkowski, A. G. Riess, The Hubble tension and early dark energy. *Annual Review of Nuclear and Particle Science* **73**, 153-180 (2023). doi: https://doi.org/10.1146/annurev-nucl-111422-024107.

23. W. Cardona, M. Kunz, V. Pettorino, Determining Ho with Bayesian hyper-parameters. *Journal of Cosmology and Astroparticle Physics* **3**, 56 (2017). doi: 10.1088/1475-7516/2017/03/056.

24. R. Cooke, F. Says, T. Andermann, T. M. Blackburn, M. J. Steinbauer, A. Antonelli, S. Faurby, Undiscovered bird extinctions obscure the true magnitude of human-driven extinction waves. *Nature Communications* **14**, 8116 (2023). doi: https://doi.org/10.1038/s41467-023-43445-2.

25. D. Silvestro, A. Kostikova, G. Litsios, P. B. Pearman, N. Salamin, Measurements errors should always be incorporated in phylogenetic comparative analysis. *Methods in Ecology and Evolution* **6**, 340-346 (2015). doi: https://doi.org/10.1111/2041-210X.12337.

26. A. R. Ives, P. E. Midford, T. Garland, Jr, Within-species variation and measurement error in phylogenetic comparative methods. *Systematic Biology* **56**, 252-270 (2007). doi: https://doi.org/10.1080/10635150701313830.

27. J. M. Beaulieu, B. C. O'Meara, P. Crane, M. J. Donoghue, Heterogeneous rates of molecular evolution and diversification could explain the Triassic age estimate for angiosperms. *Systematic Biology* **64**, 869-878 (2015). doi: https://doi.org/10.1093/sysbio/syv027

28. J. W. Brown, S. A. Smith, The past sure is tense: on interpreting phylogenetic divergence time estimates. *Systematic Biology* **67**, 340-353 (2018). doi: https://doi.org/10.1093/sysbio/syx074.

29. G. E. Budd, R. P. Mann, Two notorious nodes: a critical examination of relaxed molecular clock age estimates of the bilaterian animals and placental mammals. *Systematic Biology* In press (2023). doi: https://doi.org/10.1093/sysbio/syad057.

30. D. S. Simberloff, Taxonomic diversity of island biotas. Evolution 24, 23-47 (1970). doi: https://doi.org/10.1111/j.1558-5646.1970.tb01738.x.

31. R Core Team, R: A language and environment for statistical computing. R Foundation for Statistical Computing, Vienna, Austria (2023). https://www.R-project.org/.

32. W. M. Landau, The *targets* R package: a dynamic Make-like function-oriented pipeline toolkit for reproducibility and high-performance computing. *Journal of Open Source Software* **6**, 2959, (2021). doi: https://doi.org/10.21105/joss.02959.

33. H. Wickham, *ggplot2: Elegant Graphics for Data Analysis*. (Springer-Verlag New York, 2016).

34. E. Paradis, K. Schliep, *ape* 5.0: an environment for modern phylogenetics and evolutionary analyses in R. *Bioinformatics* **35**, 526-528 (2019). doi: https://doi.org/10.1093/bioinformatics/bty633.

35. H. Wickham H, R. François, L. Henry, K. Müller, D. Vaughan, *dplyr*: A Grammar of Data Manipulation. R package version 1.1.4 (2023). doi: https://CRAN.R-project.org/package=dplyr.

36. M. Maechler, *Rmpfr*: R MPFR - Multiple Precision Floating-Point Reliable. R package version 0.9-2 (2023). doi: https://CRAN.R-project.org/package=Rmpfr.

37. H. Wickham, D. Vaughan, M. Girlich, *tidyr*: Tidy Messy Data. R package version 1.3.1, (2024). doi: https://CRAN.R-project.org/package=tidyr.

38. S. G. Johnson, The NLopt nonlinear-optimization package (2023). https://nlopt.readthedocs.io/en/latest

39. J. D. Boyko, B. C. O'Meara, dentist: computing uncertainty by sampling points around maximum likelihood. *bioRxiv* 2023.01.10.523430 [preprint] (2023). doi: https://doi.org/10.1101/2023.01.10.523430.

40. H. Wickham, T. Pedersen, D. Seidel, *scales*: Scale Functions for Visualization. R package version 1.3.0, (2023). doi: https://CRAN.R-project.org/package=scales.

41. T. Stadler, On incomplete sampling under birth-death models and connections to the sampling-based coalescent. *Journal of Theoretical Biology* **261**, 58-66 (2009). doi: https://doi.org/10.1016/j.jtbi.2009.07.018.

42. T. Stadler, Simulating trees on a fixed number of extant species. *Systematic Biology* **60**, 676-684 (2011). doi: https://doi.org/10.1093/sysbio/syr029.

43. M. J. Sanderson, r8s: inferring absolute rates of molecular evolution and divergence times in the absence of a molecular clock. *Bioinformatics* **19**, 301-302 (2003). doi: https://doi.org/10.1093/bioinformatics/19.2.301

44. K. P. Burnham, D. R. Anderson, *Model Selection and Multimodal Inference*. (Springer Press, 2002).

45. T. Rowan, "Functional stability analysis of numerical algorithms, Thesis, University of Texas at Austin (1990).

46. M. J. D. Powell, The BOBYQA algorithm for bound constrained optimization without derivatives. (Department of Applied Mathematics and Theoretical Physics, Cambridge England, technical report NA2009/06 2009).

47. M. J. D. Powell, The NEWUOA software for unconstrained optimization without derivatives. Proc. 40th Workshop on Large Scale Nonlinear Optimization (Erice, Italy, 2004).

48. M. Steel, A. Mooers, The expected length of pendant and interior edges of a Yule tree. *Applied Mathematics Letters* **23**, 1315-1319 (2010). doi: https://doi.org/10.1016/j.aml.2010.06.021.

49. S. Nakagawa, I. C. Cuthill, Effect size, confidence interval and statistical significance: a practical guide for biologists. *Biological Reviews* **82**, 591-605 (2007). doi: https://doi.org/10.1111/j.1469-185X.2007.00027.x.

50. S. Nee, Inferring speciation rates from phylogenies. *Evolution* **55**, 661-668 (2001). doi: https://doi.org/10.1111/j.0014-3820.2001.tb00801.x.

51. J. M. Beaulieu, B. C. O'Meara, Can we build it? Yes we can, but should we use it? Assessing the quality and value of a very large phylogeny of campanulid angiosperms. *American Journal of Botany* **105**, 417-432 (2018). doi: https://doi.org/10.1002/ajb2.1020

52. J. M. Beaulieu, B. C. O'Meara, M. J. Donoghue, Identifying hidden rate changes in the evolution of a binary morphological character: the evolution of plant habit in campanulid angiosperms. *Systematic Biology* **62**, 725-737 (2013). doi: https://doi.org/10.1093/sysbio/syt034.

53. B. C. O'Meara, C. Ané, M. J. Sanderson, P. C. Wainwright, Testing for continuous trait evolution using likelihood. *Evolution* **60**, 922-933 (2006). doi: https://doi.org/10.1111/j.0014-3820.2006.tb01171.x.

54. J. M. Beaulieu, D.-C. Jhwueng, C. Boettiger, B. C. O'Meara, Modeling stabilizing selection: expanding the Ornstein-Uhlenbeck model of adaptive evolution. *Evolution* **66**, 2369-2382 (2012). doi: https://doi.org/10.1111/j.1558-5646.2012.01619.x.

55. J. M. Beaulieu, B. C. O'Meara, Detecting hidden diversification shifts in models of trait-dependent speciation and extinction. *Systematic Biology* **65**, 583-601 (2016). doi: https://doi.org/10.1093/sysbio/syw022.

Acknowledgments: This work presented here was substantially influenced by James Boyko's advocacy in challenging the artifactual nature of age rate scaling. Conversations with Dan Simberloff, Nina Fefferman, Paul Armsworth, Xingli Giam, Naomi O'Meara, Adam Siepielski, and Andy Alverson were also of substantial help in generating ideas and providing constructive feedback.

Funding:

National Science Foundation grants DEB−1916539 (BCO)

National Science Foundation grants DEB−1916558 (JMB)

Author contributions:

Project conceptualization and planning: BCO, JMB

Methodology: BCO, JMB

Investigation: BCO, JMB

Funding acquisition: BCO, JMB

Writing – review and editing: BCO, JMB

Competing interests: The authors declare that they have no competing interests.

Data and materials availability: All scripts and substantial outputs are available at https://github.com/bomeara/hyperbolic_rates.

Supplementary Materials

Materials and Methods

Figs. S1 to S10

Tables S1

References (*31–55*)

Movie S1

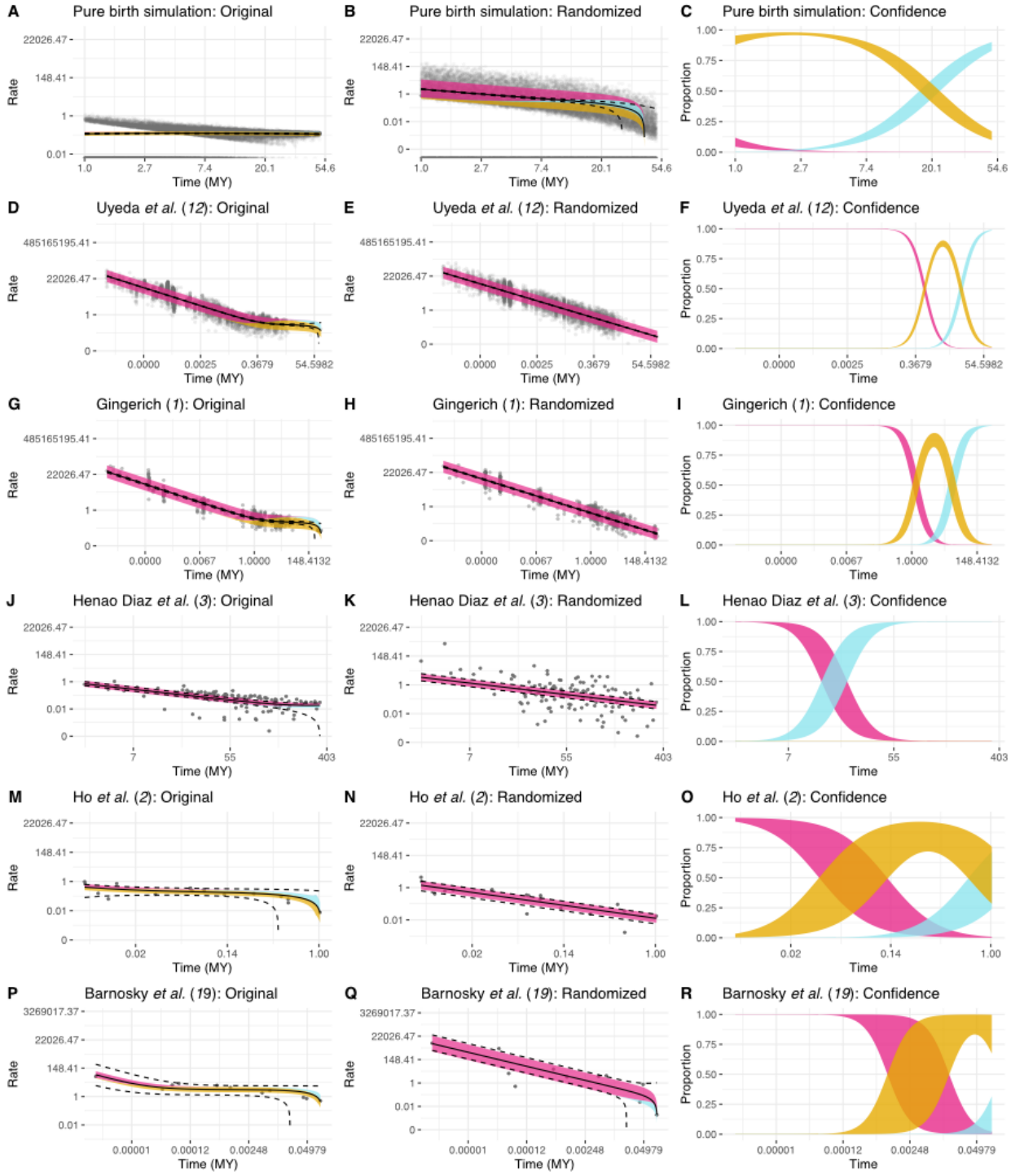
A
Pure birth simulation: Original
B
Pure birth simulation: Randomized
C
Pure birth simulation: Confidence
D
Uyeda et al. (12): Original
E
Uyeda et al. (12): Randomized
F
Uyeda et al. (12): Confidence
G
Gingerich (1): Original
H
Gingerich (1): Randomized
I
Gingerich (1): Confidence
J
Henao Diaz et al. (3): Original
K
Henao Diaz et al. (3): Randomized
L
Henao Diaz et al. (3): Confidence
M
Ho et al. (2): Original
N
Ho et al. (2): Randomized
O
Ho et al. (2): Confidence
P
Barnosky et al. (19): Original
Q
Barnosky et al. (19): Randomized
R
Barnosky et al. (19): Confidence
Rate
Proportion
Time (MY)
Time

Fig. 1. Comparisons of log-linear trends in evolutionary rates: simulated data vs. empirical studies. While simulated data exhibit constant birth rates through time, empirical datasets consistently reveal a significant negative correlation between rate and time. The first column is for the original data; the second column is using the randomization procedure. Time is plotted along the horizontal axis, and rate (log-scaled) along the vertical axis. Individual rate estimates are depicted as dots, with a black line representing regression from the best fitting model, and dashed lines indicating the 95% confidence interval around the regression. Additionally, the thick line illustrates the relative impact of the various components from our least-squares model on the overall rate in the best fitting model: dark pink represents the hyperbolic component (which appears linear on this log-log plot), goldenrod denotes a constant rate component, and blue signifies a linear component. Note that for the pure birth simulation there are some rates that are zero, which are placed at negative infinity on a log scale. Finally, the third column illustrates the proportion of the rate from each model component over time, with band thickness indicating uncertainty in that proportion.

5

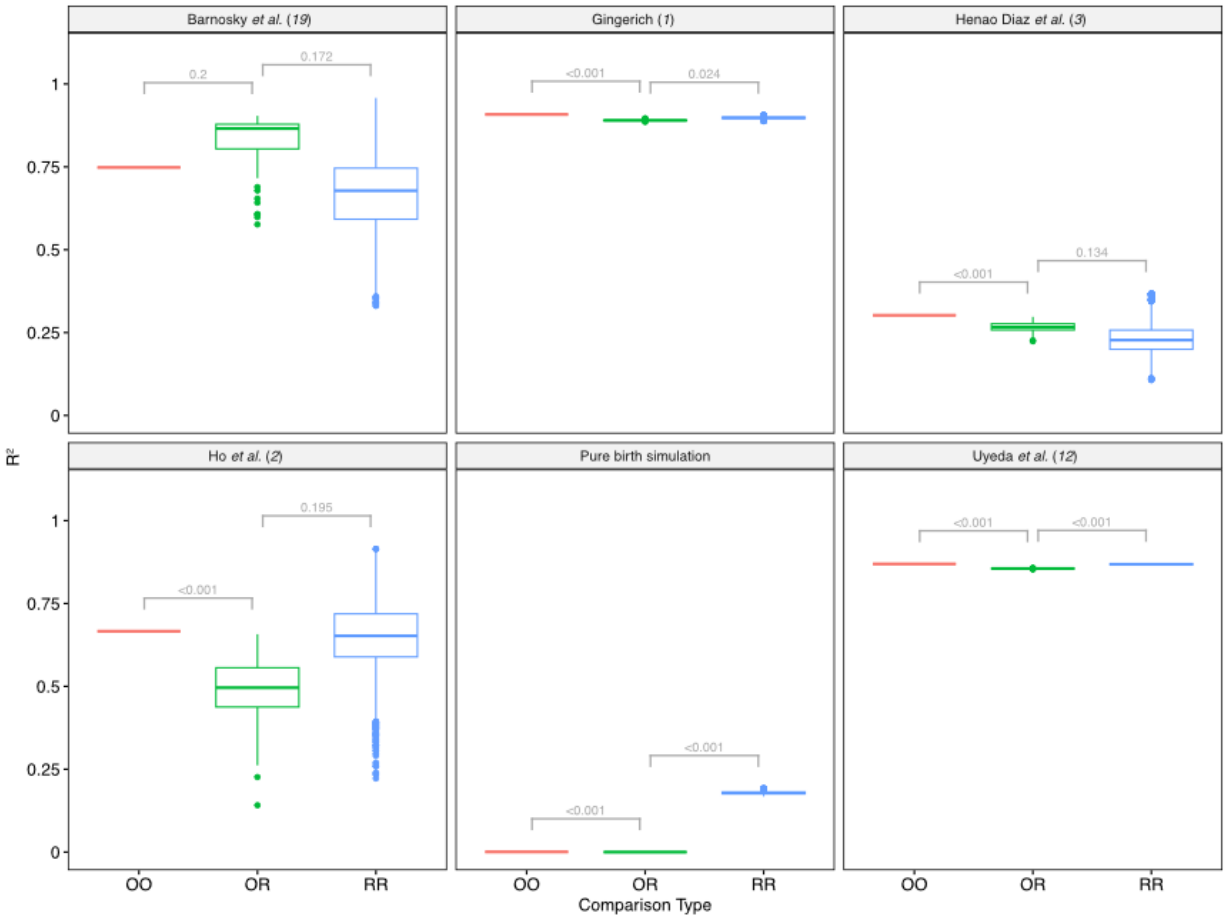

Fig. 2. Comparisons of coefficient of determination (R^2) between the observed fit and fits from randomizing the numerator relative to the denominator of the empirical rates. First, obtained the R^2 of the empirical original (O) data fit to the original (O) parameters (comparison type OO). Second, we evaluated the predictive accuracy of the parameters estimated from resampled data applied back to the original empirical data. This involved first separating each empirical rate into its numerator and denominator components, shuffling the numerators at random across a given empirical dataset, and then divided them by the unshuffled times to obtain a new set of rates and times, repeated 100 times. We then compared the fit of the empirical original data to predictions from the randomized data (comparison type OR). This allowed us to see how much the random data predicts the original data. It is possible that, even if the original data were pure noise, the fit would still be worse when using a different randomized dataset since it was not tuned to the focal dataset. To check this, we also computed the R^2 between a randomized dataset and the fitted values from a different randomized dataset (RR comparison type).